A New Accurate Analytical Expression for the SiPM Transient Response to Single Photons

D. Marano, G. Bonanno, M. Belluso, S. Billotta, A. Grillo, S. Garozzo, G. Romeo
INAF (Istituto Nazionale di Astrofisica) – Osservatorio Astrofisico di Catania
Via Santa Sofia 78, I-95123 Catania, Italy
E-mails: [dmarano, gbonanno, mbelluso, sbillotta, agrillo, sgarozzo, gromeo]@oact.inaf.it

A. D. Grasso, S. Pennisi, G. Palumbo
DIEEI (Dipartimento di Ingegneria Elettrica, Elettronica e Informatica) – Università di Catania
Viale Andrea Doria 6, I-95125 Catania, Italy
E-mails: [agrasso, gpalumbo, spennisi]@dieei.unict.it

***Abstract* — In this paper a comprehensive analytical analysis is performed based on a new accurate electrical model of silicon photomultiplier (SiPM) detectors. The proposed circuit model allows to accurately reproduce the SiPM output time response regardless of the particular technology adopted for the fabrication process, and can also be profitably exploited to perform reliable circuit-level simulations. A novel expression of the detector photoelectron response due to a single photon absorption is systematically developed. The obtained waveform accurately reproduces the fast detector ignition, the ensuing avalanche self-quenching and the final slow recharging operation. Predictive capabilities of the adopted analytical model are demonstrated by means of experimental measurements on a real SiPM device.**

***Index Terms* — Analytical functions, electrical model, SiPM, small-signal analysis, time constants, transient response.**

I. INTRODUCTION

Silicon photomultipliers (SiPMs), also referred to as multi-pixel photon counters (MPPCs), are a favourable class of semiconductor-based photodetectors addressing the challenge of detecting, timing and quantifying low-light optical signals down to the single-photon counting level. SiPMs offer a highly attractive alternative that closely mimics the low-light detection capabilities of traditional photomultiplier tubes, while providing all the benefits of a solid-state device.

The extremely remarkable performance achieved by SiPM sensors in terms of high photon detection efficiency, fast transient response, excellent timing resolution, and wide spectral range, has made considerable research activities and technological development to be constantly devoted to SiPM devices within the scientific community involved in medical imaging, high-energy physics and astrophysics. Contextually, the electronics development aims at the realization of specifically designed front-end architectures to acquire, preserve and reproduce the SiPM output electrical signals.

Essential prerequisite for a successfully designed read-out configuration is an accurate equivalent electrical model of the SiPM detector allowing a reliable interpretation of its physical interactions with the conditioning electronics. A careful theoretical study of both static and dynamic characteristics of the silicon detector as a signal source is therefore required to help choose the most performing front-end solutions. In this scenario, the availability of a truthful analytical expression of the SiPM response, along with the possibility of performing reliable circuit-level simulations, becomes a key point of the design phase, since the main characteristics of the achieved functions can be profitably related to the model parameters of both SiPM detectors and front-end electronics. In addition, on the basis of this analytical model, the core physical properties of SiPMs can be functionally related to the equivalent circuit parameters regardless of the specific fabrication technology.

This work develops a detailed analytical investigation of an accurate electrical model of the SiPM detectors. Although different SiPM electrical characterizations are reported in literature, analytical research studies of the adopted models are still few [1]-[8]. A new accurate analytical expression for the single-photoelectron response is derived and discussed. Compared to other reported models, the present work mostly focuses on a detailed analytical investigation of the SiPM model aimed at achieving a simple and accurate expression of the SiPM output pulse response. Functional relationships are here provided for the most crucial model parameters, and the associated curve plots are critically analyzed. SPICE simulations and experimental measurements on a real device corroborates the achieved analytical expressions.

II. SIPM ELECTRICAL MODEL

The equivalent model simulating the discharge of N_f active microcells for a SiPM detector consisting of a total number of N microcells is depicted in Fig. 1. The circuit is separated into an active component for the N_f fired pixels and a passive part for the remaining N_p=N-N_f unfired microcells.

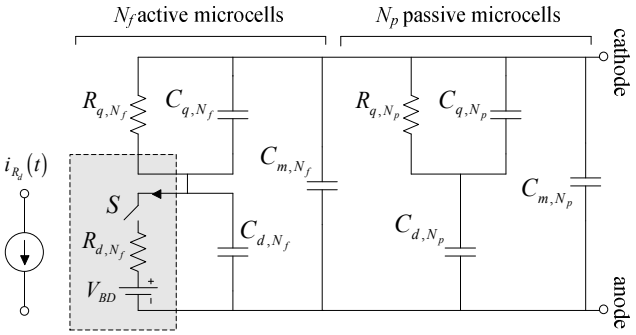

Fig. 1. SiPM equivalent electrical model. The circuit branch in the dashed box, mimicking the avalanche discharges of the firing microcells, can be opportunely replaced by a proper time-dependent current generator.

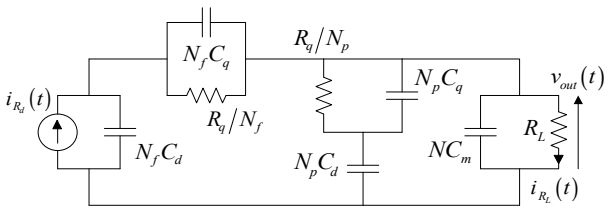

Fig. 2. SiPM small-signal equivalent model with a passive read-out circuit.

For each individual pixel, R_d is the internal resistance of the diode space-charge and quasi-neutral regions, C_d is the junction capacitance of the inner depletion layer, R_q and C_q are the integrated quenching resistance and parallel stray capacitance, respectively, and C_m accounts for all parasitic capacitive contributions across the two pixel terminals. A further fringe capacitance for the common cathode bonding pad should be also included in the model, but its effects can be endorsed in the parallel contribution of C_m for each microcell.

The i-th equivalent resistances and capacitances included in the model are expressed by the following relationships

$$R_{i,N_f}=\frac{R_i}{N_f},\ R_{i,N_p}=\frac{R_i}{N_p},\ C_{i,N_f}=N_f C_i,\ C_{i,N_p}=N_p C_i \quad (1)$$

The avalanche discharge of the firing cells can be modeled by a DC voltage supply representing the diode breakdown potential, V_{BD}, in series with a voltage-controlled switch, S. This branch can be more conveniently replaced by a proper time-dependent current source representing the instantaneous current, $i_{Rd}(t)$, flowing through the equivalent diode resistance $R_{d,Nf}$, as sketched in the dashed box in Fig. 1.

The advantage of the latter avalanche generation model relies in the possibility of achieving a comprehensive analytical expression of the SiPM output response accurately describing all characteristic transient phases resulting from a trigger ignition (by photon absorption or thermic generation).

III. Small-signal analysis

Fig. 2 depicts the linearized small-signal equivalent circuit used for deriving the Laplace-domain analytical expression of the SiPM output current $i_{RL}(t)$ across a resistive load R_L, representing the equivalent input resistance of the front-end electronics. The circuit directly results from the model in Fig. 1 by inverting the direction of the input source and output current and grouping capacitors $C_{m,Nf}$ and $C_{m,Np}$ into the single equivalent contribution $C_{m,N}=NC_m$.

The complete small-signal transfer function of the circuit in Fig. 2 as a function of the complex frequency is found to be

$$H(s)=\frac{I_{R_L}(s)}{I_{R_d}(s)}=\frac{1+b_1' s+b_2' s^2}{1+a_1' s+a_2' s^2+a_3' s^3} \quad (2)$$

where the s-coefficients in the numerator are given by

$$b_1'=R_q\left(C_d+2C_q\right) \quad (3)$$

$$b_2'=R_q^2 C_q\left(C_d+C_q\right) \quad (4)$$

while those in the denominator are expressed by

$$a_1'=2R_q\left(C_d+C_q\right)+NR_L\left(C_d+C_m\right) \quad (5)$$

$$a_2'=R_q\left[R_q\left(C_d+C_q\right)^2+NR_L\left(C_d^2+2C_dC_q+2C_mC_d+2C_mC_q\right)\right] \quad (6)$$

$$a_3'=NR_LR_q^2\left(C_d+C_q\right)\left[C_dC_q+C_m\left(C_d+C_q\right)\right] \quad (7)$$

Collecting both numerator and denominator of (2), an exact pole-zero cancellation occurs, leading to

$$H(s)=\frac{1+sR_q\left(C_d+C_q\right)}{1+sR_q\left(C_d+C_q\right)}\frac{1+b_1 s}{1+a_1 s+a_2 s^2}=\frac{1+b_1 s}{1+a_1 s+a_2 s^2} \quad (8)$$

where $b_1=R_qC_q$, and the s-coefficients in the denominator are

$$a_1=R_q\left(C_d+C_q\right)+NR_L\left(C_d+C_m\right) \quad (9)$$

$$a_2=NR_LR_q\left(C_dC_q+C_dC_m+C_qC_m\right) \quad (10)$$

Since $a_1^2>4a_2$ upon any values of the passive elements, the above transfer function exhibits two real poles and can hence be more conveniently expressed as

$$H(s)=\frac{1+sR_q\left(C_d+C_q\right)}{1+sR_q\left(C_d+C_q\right)}\frac{1+b_1 s}{1+a_1 s+a_2 s^2}=\frac{1+b_1 s}{1+a_1 s+a_2 s^2} \quad (11)$$

in which $\tau_z=b_1$, while the associated time constants are related to the denominator s-coefficients according to

$$\tau_{p1}=\left(a_1+\sqrt{a_1^2-4a_2}\right)\Big/2 \quad (12)$$

$$\tau_{p2}=\left(a_1-\sqrt{a_1^2-4a_2}\right)\Big/2 \quad (13)$$

As far as the input current generator is concerned, the total charge released by the avalanche events, as turns out from the physics theory of the device, is instantly collected across the equivalent resistance $R_{d,Nf}$, and results in a photodiode current $i_{Rd}(t)$ which abruptly jumps to its peak value, dictated by the excess bias voltage V_{OV} beyond breakdown, and exponentially drops with a circuit-dependent decay time constant. Thus

$$i_{R_d}(t)=I_0\, e^{-\frac{t}{\tau_d}} \quad (14)$$

where I_0 represents the current peak value given by

$$I_0=\frac{V_{OV}}{R_{d,N_f}}=N_f\frac{V_{OV}}{R_d} \quad (15)$$

and τ_d is the quenching time constant set by [2], [4]

$$\tau_d=\left(R_{d,N_f}\|R_{q,N_f}\right)\left(C_{d,N_f}\|C_{q,N_f}\right)=\frac{R_dR_q}{R_d+R_q}\left(C_d+C_q\right) \quad (16)$$

which, typically being $R_d \ll R_q$, can be approximated by

$$\tau_d\approx R_d\left(C_d+C_q\right) \quad (17)$$

Since the photodiode avalanche current is merely related to the charge delivered by the firing microcells, the above

$i_{Rd}(t)$ expression, owing to the superposition principle, is then helpfully exploited to model the general case in which more than one pixel is interested by an avalanche event.

Integrating the photodiode current in (14) over time, yields the overall charge delivered by the fired microcells

$$Q = \int_0^{+\infty} i_{R_d}(t)\,dt = I_0 \tau_d \tag{18}$$

from which, considering the charge due to a single fired pixel (assuming N_f=1), yields the commonly adopted expression for the SiPM gain G as a function of the applied overvoltage V_{OV} and total microcell capacitance C_d+C_q

$$G = \frac{Q|_{N_f=1}}{e} = \frac{V_{OV}\left(C_d + C_q\right)}{e} \tag{19}$$

It should be noted that previously reported SiPM electrical circuits adopting the input current generator as a Dirac's delta pulse to simulate the trigger avalanche discharge might be inherently limited for an accurate modeling of all characteristic features of the output pulse in response to a detected event.

Explicating the SiPM output current in (2), yields

$$I_{R_L}(s) = H(s)\, I_{R_d}(s) \tag{20}$$

where the Laplace transform of the photodiode current is

$$I_{R_d}(s) = L\left\{i_{R_d}(t)\right\} = I_0 \frac{\tau_d}{1+s\tau_d} \tag{21}$$

Substituting expressions (11) and (21) into (20), gives

$$I_{R_L}(s) = I_0 \tau_d \frac{1+s\tau_z}{\left(1+s\tau_d\right)\left(1+s\tau_{p1}\right)\left(1+s\tau_{p2}\right)} \tag{22}$$

from which, by inverse Laplace transforming, the complete SiPM output current can be derived as a function of time

$$i_{R_L}(t) = I_0 \tau_d \left(A_d\, e^{-\frac{t}{\tau_d}} + A_{p1}\, e^{-\frac{t}{\tau_{p1}}} + A_{p2}\, e^{-\frac{t}{\tau_{p2}}} \right) \tag{23}$$

with the three exponentials coefficients being given by

$$A_d = \frac{\tau_d - \tau_z}{\left(\tau_d - \tau_{p1}\right)\left(\tau_d - \tau_{p2}\right)} \tag{24}$$

$$A_{p1} = \frac{\tau_{p1} - \tau_z}{\left(\tau_{p1} - \tau_d\right)\left(\tau_{p1} - \tau_{p2}\right)} \tag{25}$$

$$A_{p2} = \frac{\tau_{p2} - \tau_z}{\left(\tau_{p2} - \tau_d\right)\left(\tau_{p2} - \tau_{p1}\right)} \tag{26}$$

Since τ_d<τ_{p2}<τ_z<τ_{p1} for feasible values of the circuit model parameters, it follows A_d<0 and A_{p1}, A_{p2}>0.

The complete SiPM time domain response is thus a triple-exponential function consisting of three succeeding intervals, rising, quenching and recovery, reflecting the physical processes undergone by the generated avalanche discharge across the SiPM output terminals. Each of the aforementioned phase is associated with a relevant circuit time constant.

The rising phase (τ_d) corresponds to the time required by an avalanche discharge to be transferred to the read-out load; the quenching phase (τ_{p2}) accounts for the voltage drop across the quenching resistance; the recovery phase (τ_{p1}) originates from the slow recharging of the equivalent diode capacitances.

The charge injected by the fired pixels, represented by the integral of the photodiode current in (18), is delivered as a current signal through the read-out resistor for the entire output pulse duration. In other words, the surface area underneath the output current curve is equivalent to that lying beneath the photodiode current. Indeed, integrating (23) with respect to time, leads to the same expression as in (18).

To perform a first-order analytical assessment of time constants τ_{p1} and τ_{p2} and provide a graphical comparison with the related curve plots, by comparing the denominators in (8) and (11) yields a_1=τ_{p1}+τ_{p2} and a_2=$\tau_{p1}\tau_{p2}$, from which, assuming τ_{p2} ≪τ_{p1}, leads to τ_{p1}≈a_1 and τ_{p2}≈a_2/a_1. Moreover, neglecting the small contribution of C_m, τ_{p1} and τ_{p2} further simplify into

$$\tau_{p1} \approx R_q\left(C_d + C_q\right) + NR_L C_d \tag{27}$$

$$\tau_{p2} \approx \frac{NR_L R_q C_d C_q}{R_q\left(C_d + C_q\right) + NR_L C_d} \tag{28}$$

Time constant τ_{p1} is considered as one of the most significant parameters of the SiPM response, since it defines the recovery time of the diode microcells.

Fig. 3 and Fig. 4 depict the analytical behavior of the complete and approximated expressions of τ_{p1} and τ_{p2}, respectively in (12)-(13) and in (27)-(28), as a function of the total number of cells, N, and for feasible values of the passive elements.

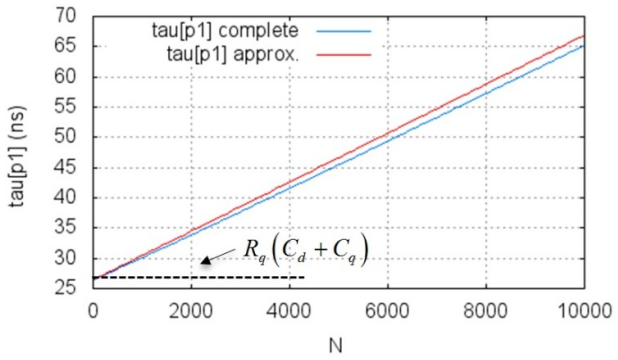

Fig. 3. Recovery time constant of the SiPM output current on a 50-Ω load as a function of N (R_d=1kΩ, R_q=300kΩ, C_d=80fF, C_q=10fF, C_m=1fF).

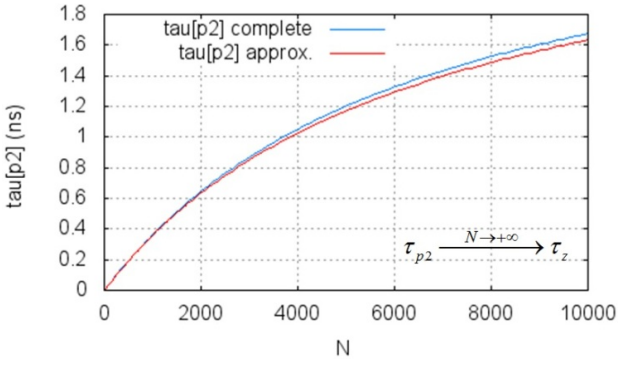

Fig. 4. Quenching time constant of the SiPM output current on a 50-Ω load as a function of N (R_d=1kΩ, R_q=300kΩ, C_d=80fF, C_q=10fF, C_m=1fF).

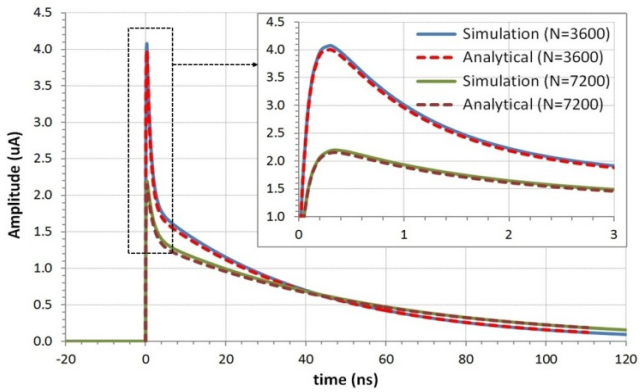

Fig. 5. Analytical and simulated SiPM single-photoelectron output current waveforms, for V_{OV}=0.8V and two different values of N.

By direct inspection of the above plots, it turns out that the quenching time constant presents a roughly hyperbolic behavior with increasing N, approaching to the constant value of τ_z. On the other side, the recovery time constant almost linearly rises with N from the initial value $R_q(C_d+C_q)$.

IV. Model Validation

To verify the accuracy of the achieved expressions, SPICE simulations are performed for the proposed equivalent model. Analytical and simulated output current pulses for the same circuit parameters are compared in Fig. 5 for two values of N.

As expected, with increasing values of N, the single output current pulse decreases its peak current and enlarges the associated time constants while keeping the same time integral, in good agreement with the obtained functions.

Analytical and measured output pulse waveforms are compared for a 3x3mm^2 50-µm Hamamatsu device. Tests are performed on the assembled read-out circuit in Fig. 6. SiPM time responses are captured with the detector in dark.

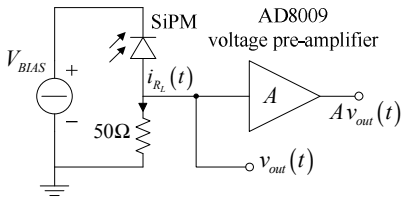

Fig. 6. Schematic overview of the SiPM read-out circuit.

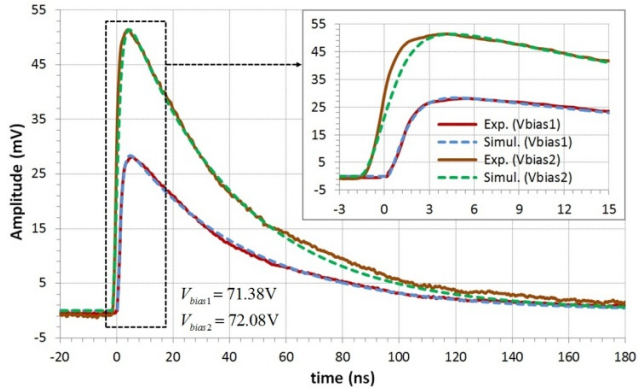

Fig. 7. Simulated and experimental (averaged) output single-photoelectron responses on a 50-Ω load resistor, for N=3600 and two different V_{OV} values.

TABLE I
ESTIMATED MICROCELL MODEL PARAMETER VALUES

SiPM S/N	Hamamatsu S11828-3344MX				
Parameter	R_d (Ω)	R_q (Ω)	C_d (F)	C_q (F)	C_m (F)
Values	1k	290k	78f	8f	1f

Circuit model parameters of the Hamamatsu device are estimated based on experimental measurements and the extracted values are summarized in Table I. Parameters extraction is accomplished through a dedicated characterization procedure [9]-[10]. Measures are performed at 25°C, at which a breakdown voltage of 70.5V is obtained.

The adopted electrical circuit of the SiPM detector is simulated, with the SPICE model of the voltage pre-amplifier included in the simulation scheme cascaded to the output load, to account for the frequency shaping in the rising edge of the measured signal (due to the limited amplifier bandwidth).

For a single firing cell, data outputs of both simulated and measured output voltage pulses are merged together in Fig. 7 for N=3600 at different overvoltages (0.88V and 1.58V) and for a 36-dB pre-amplifier gain. Simulated and experimental curves are well-matched, validating the above analysis.

IV. Conclusions

A systematic theoretical analysis of an accurate SiPM electrical model is carefully addressed to reproduce and predict the SiPM output response. The adopted model allows for an accurate analytical analysis of the detector behavior. Measurement results validate the accuracy of the analytical expressions.

References

[1] G. Condorelli, *et al.*, "Extensive Electrical Model of Large Area Silicon Photomultipliers", *Nucl. Instr. and Meth. in Phys. Res. A*, vol. 654, pp. 127-134, 2011.

[2] N. Pavlov, G. Mæhlum, D. Meier, "Gamma Spectroscopy Using a Silicon Photomultiplier and a Scintillator", *Proc. IEEE Nucl. Science Symp. Conf. Record*, pp. 173–180, 2005.

[3] S. Seifert, *et al.*, "Simulation of Silicon Photomultiplier Signals", *IEEE Trans. on Nucl. Science*, vol. 56, no.6, pp. 3726-3733, 2009.

[4] F. Corsi, *et al.*, "Electrical Characterization of Silicon Photomultiplier Detectors for Optimal Front-End Design", *Proc. IEEE Nucl. Science Symp. Conf. Record*, pp. 1276-1280, 2006.

[5] A. K. Jha, H. T. van Damm, M. A. Kupinski, E. Clarkson, "Simulating Silicon Photomultiplier Response to Scintillation Light", *IEEE Trans. on Nucl. Science*, vol. 60, no.1, pp. 336-351, 2013.

[6] D. Marano, *et al.*, "Improved SPICE Electrical Model of Silicon Photomul-tipliers", *Nuclear Instruments and Methods in Physics Research A*, vol. 726, pp. 1-7, 2013.

[7] D. Marano, *et al.*, "Silicon Photomultipliers Electrical Model Extensive Analy-tical Analysis", *IEEE Transactions on Nuclear Science*, vol. 61, no. 1, pp. 23-34, 2013.

[8] G. Giustolisi, G. Palumbo, P. Finocchiaro, A. Pappalardo," A Simple Extraction Procedure for Determining the Electrical Parameters in Silicon Photomultipliers", *Proc. IEEE ECCTD*, pp. 1-4, 2013.

[9] G. Bonanno, *et al.*, "Characterization Measurements Methodology and Instrumental Set-up Optimization for new SiPM Detectors - Part I: Electrical Tests", *IEEE Sensors Journal*, vol. 14, no. 10, pp. 3557-3566, 2014.

[10] G. Bonanno, *et al.*, "Characterization Measurements Methodology and Instrumental Set-up Optimization for new SiPM Detectors - Part II: Optical Tests", *IEEE Sensors Journal*, vol. 14, no. 10, pp. 3567-3578, 2014.